REVIEW OF SCIENTIFIC INSTRUMENTS **88**, 063901 (2017)

Chamber for mechanical testing in H_2 with observation by neutron scattering

Matthew Connolly,[a] Peter Bradley,[b] Andrew Slifka,[c] and Elizabeth Drexler[d]
Applied Chemicals and Materials Division, Material Measurement Laboratory, National Institute of Standards and Technology, 325 Broadway, Boulder, Colorado 80305, USA

(Received 27 March 2017; accepted 4 June 2017; published online 27 June 2017)

A gas-pressure chamber has been designed, constructed, and tested at a moderate pressure (3.4 MPa, 500 psi) and has the capability of mechanical loading of steel specimens for neutron scattering measurements. The chamber will allow a variety of *in situ* neutron scattering measurements: in particular, diffraction, quasielastic scattering, inelastic scattering, and imaging. The chamber is compatible with load frames available at the user facilities at the NIST Center for Neutron Research and Oak Ridge National Laboratory Spallation Neutron Source. A demonstration of neutron Bragg edge imaging using the chamber is presented. [http://dx.doi.org/10.1063/1.4986471]

I. INTRODUCTION

The primary motivation for the combined gas- and mechanical-loading chamber described in this paper is to study the effect of hydrogen embrittlement in steels. With hydrogen embrittlement, steels lose ductility and exhibit fatigue crack growth rates (FCGRs) 10–100 times larger in a H_2 environment compared to air.[1–5] Because of the fast diffusion of H_2 from the steels, the effect of hydrogen embrittlement presents only during exposure, and steel specimens will exhibit in-air fatigue crack growth rates shortly after being removed from a hydrogen environment (≈45 min).[6] Thus, any measurements designed to study hydrogen embrittlement and hydrogen-enhanced fatigue crack growth must be performed *in situ*.

The study of hydrogen embrittlement and hydrogen-assisted fatigue crack growth is ripe for the use of neutron scattering techniques. As hydrogen scatters neutrons particularly strongly, the measurement of neutron radiographs during an FCGR measurement is one of the only techniques that can provide information about hydrogen distribution and the density of hydrogen near a crack tip.[7] Quasi-elastic neutron scattering can provide dynamic information on the diffusion rates of hydrogen through materials.[8] Inelastic neutron scattering measures phonon spectra, allowing for a direct measurement of the effect of hydrogen intercalation on the Fe–Fe bond strength.[9] Obtaining this information during FCGR measurements is required to fully understand the mechanisms of hydrogen-assisted fatigue crack growth and, perhaps, hydrogen embrittlement and crucial to the validation of existing modeling efforts and the development of more advanced models.[10]

FCGRs are measured according to the ASTM E647-15 standard.[11] The differential crack extension per fatigue cycle, da/dN, is measured as a function of ΔK, the stress intensity factor range, as determined from linear elastic stress analysis. The test involves cyclic loading of a notched specimen which has been fatigue pre-cracked. The crack size is calculated by compliance throughout the test from a clip gauge at the load line, and the data are analyzed to give the differential crack extension per fatigue cycle. For $\Delta K \gtrsim 12$ MPa$\sqrt{\text{m}}$, typical FCGRs in pipeline steel are on the order of 10^{-5} mm/cycle in air and 10^{-4} mm/cycle to 10^{-3} mm/cycle in H_2.

Thus, a chamber is required that is compatible with the load frames necessary for FCGR measurements, which will also allow for sufficient transmission of neutron radiation through the chamber walls. Load frames suitable for performing fatigue crack growth rate measurements are offered as ancillary equipment at beam lines at the NIST Center for Neutron Research[12] and Oak Ridge National Laboratory's Spallation Neutron Source[13] user facilities. Two chambers for FCGR measurements in high-pressure hydrogen are currently in use at the H_2 facility at NIST, Boulder.[1,14] These chambers, unfortunately, have 5.1 cm (2 in.) thick walls made of steel, which prohibit their use in neutron scattering measurements.

Gas-pressure cells for neutron scattering applications have been developed which use high-strength aluminum alloys, Ti–Zr, and $CuBe_2$[15] as chamber materials. Ti and Zr have coherent scattering lengths of opposite signs,[16] providing a route for producing a Ti–Zr composite material with an overall coherent scattering cross section of zero, so that any Bragg peaks due to the chamber walls are eliminated. These materials do scatter incoherently, however, raising the background scattering levels above those desirable for phonon measurements. Ti and Zr also have high atomic numbers and, therefore, large electron densities, which would limit potential future x-ray scattering applications of the chamber. $CuBe_2$ has a high yield strength (1140 MPa–1450 MPa),[17] ideal for producing strong chambers. However, Be is a strong absorber of neutrons, which increases the attenuation due to the chamber.

[a]matthew.connolly@nist.gov
[b]peter.bradley@nist.gov
[c]andrew.slifka@nist.gov
[d]elizabeth.drexler@nist.gov

The scattering of neutrons from aluminum is nearly entirely coherent, and therefore the incoherent scattering background is very low. The coherent scattering length of aluminum is small, and the overall attenuation is small for even moderately thick chamber walls. Further, scattering spectra of the empty chamber can be subtracted from the spectra with a specimen in order to remove Bragg peaks in the diffraction pattern attributable to the aluminum chamber. This type of post-processing correction is much easier to deal with than the effect of a large incoherent scattering background.

We are unaware of any other chambers used in neutron scattering measurements that allow for cyclic mechanical loading in a controlled gas environment.

II. CHAMBER DESIGN

A. Design restrictions

The design of the chamber was directed by conversations with neutron facilities, in order to ensure proper design for user facility load frames and other experimental apparatus. The main requirements for the design of the hydrogen chamber are as follows:

- to allow operation pressures up to 3.4 MPa (500 psi) with minimal leak rates;
- to allow for cyclic actuation of a pull rod while maintaining those minimal leak rates;
- to allow tensile loads on the specimen up to 3.5 kN;
- to be sufficiently transparent to neutrons to allow for feasible experiments;
- to be compact, so as to fit in load frames and sample stages that are available at leading neutron sources; and
- to encompass appropriate measures to protect the chamber and facility from the following:
  - (a) rapid escape of gas during operation;
  - (b) premature pullout/failure of load train connections; and
  - (c) over stroke and/or overload resulting from controller errors.

Because the H_2 gas which leaks from the chamber seals can be vented either to a flammable gas exhaust system or simply directed upwards and away from the experimental equipment in a controlled manner, there is no hard limit on the H_2 leak rate. However, for safety considerations, it is desirable for the leak rate to be sufficiently low as to keep the total amount of H_2 required below an amount which could reach the Lower Explosive Limit (LEL). This would prevent the combustion of H_2 even in the event of a catastrophic loss of gas from the supply bottle. For H_2, the LEL is 4%.[18] A typical experiment at a neutron facility will last on the order of 5 days, and the chamber will be used in an experiment area with total volume on the order of 200 m^2 or larger. Under these conditions, any leak rate lower than 0.61 MPa/h will ensure that even at a catastrophic loss of gas from the supply bottle, the concentration of H_2 will never be larger than one tenth of the LEL for H_2.

The chamber was designed to accommodate compact tension [C(T)] specimen geometries; however, only slight modifications to the load train and clevises would be required to accommodate other geometries. Specific geometric restrictions are that the chamber be no taller than 41 cm and have an outer wall diameter less than 100 mm. The height limitation is required for the chamber to fit in the load frames available at the neutron sources. The outer wall diameter is a limitation that is directed by the position of detectors and collimation slits.

To be sufficiently transparent to neutrons, the chamber was constructed of the aluminum alloy 6061-T6 (AA6061-T6). AA6061-T6 was chosen over other aluminum alloys, as it is commonly used for neutron scattering experiments because of its high strength and minimal attenuation of a neutron beam. The major alloying elements of AA6061-T6 are magnesium and silicon, neither of which becomes significantly activated in a neutron beam.

For safe operation, conservative design practices were employed to ensure integrity of the chamber during normal operation. Engineering design controls were implemented to prevent large pressure excursions in the event of a seal or chamber failure. To this end, the chamber is intended for the moderate pressure operation of 3.4 MPa (500 psi). Dual U-cup seals along the pull rod were employed and a vent line above the upper U-cup seal was implemented. Additionally, design-for-failure methodology was employed at the critical attachment/connections, such as the connecting studs between the chamber and load cell, the pull rod, and the chamber to load frame.

We ensured adequate thread pullout strengths of the connecting studs for the projected operating loads. This required managing the load path to prevent over stroke or compression of the pull rod, either upon completion of the test or during setup. Two nuts, one at the top of the pull rod and a second at the bottom, below the end cap, act as stroke limiters. The stroke limiter at the top of the pull rod prevents over-compression, which could result in loss of the integrity of the seal. The stroke limiter just below the end cap was implemented in order to prevent damage due to an over stroke. In the event of an over stroke, the bottom stroke limiter ensures that the load transfers to the end cap of the chamber, preventing seal loss, and then to the base where the chamber is attached to the load frame. The aluminum step stud attaching the chamber to the load frame is designed as the failure point, such that the step stud will pull out in the event of an over stroke, protecting the integrity of the chamber and load frame to ensure a safe failure mode.

B. Design calculations

1. Pressure

The minimum wall thickness was calculated by assuming that the chamber is an infinite cylinder, and a significant safety factor was included to account for any underestimations from this assumption. AA6061-T6 has a yield strength of 275 MPa. The stresses exerted by an internal pressure in an infinitely long cylinder are given by

$$\sigma_r = \frac{r_1^2 r_2^2 (p_2 - p_1)}{r_2^2 - r_1^2}\frac{1}{r^2} + \frac{r_1^2 p_1 - r_2^2 p_2}{r_2^2 - r_1^2},$$
$$\sigma_\theta = -\frac{r_1^2 r_2^2 (p_2 - p_1)}{r_2^2 - r_1^2}\frac{1}{r^2} + \frac{r_1^2 p_1 - r_2^2 p_2}{r_2^2 - r_1^2}, \text{ and} \tag{1}$$
$$\sigma_z = \nu(\sigma_r + \sigma_\theta),$$

where $\nu = 0.33$ is Poisson's ratio for AA6061-T6, p_1 and p_2 are the inner and outer pressures, respectively, and r_1 and r_2 are the inner and outer radii of the cylinder, respectively.[19] The wall thickness, t, is then given by

$$t = r_2 - r_1. \tag{2}$$

The stresses are added in quadrature, and a safety factor included according to

$$\frac{\text{Yield Strength}}{\text{Safety Factor}} = \sqrt{\sigma_r^2 + \sigma_\theta^2 + \sigma_z^2}. \tag{3}$$

With an internal diameter of 7.6 cm, an external pressure of 0 MPa, an internal pressure of 3.4 MPa, and a safety factor of 4, the solution to Eq. (3) gives a required outer diameter of 8 cm. The minimum required wall thickness is, therefore, $t = 2$ mm.

2. Beam transmission

In addition to being structurally sound, we must ensure sufficient transmission of neutrons through the chamber walls. The transmission of radiation through a material is given by the Beer-Lambert law,

$$T = e^{-\mu L}, \tag{4}$$

where μ is the linear attenuation coefficient[20,21] of the material ($\mu = 0.0031$ mm^{-1} for Al with 4 Å neutrons) and L is the distance through which the material travels. Here, $L = 2t$ to account for the attenuation as the incident beam enters the chamber and the attenuation as the scattered beam exits the chamber. At t = 3.2 mm (1/8 in.), neutrons are attenuated only ≈2%. These attenuation levels are sufficiently low for the proposed experiments.

3. Thread pull-out

The chamber is attached to the base of a load frame by a threaded step stud. The load chain is attached to the chamber by another step stud. As the chamber is made from AA6061-T6, the capacity of the threads of the chamber must be ensured to withstand the operating loads to prevent strip or pull-out during operation. In the case of the chamber attachment to the load frame and attachment of the load train to the chamber, it must also have sufficient strength to prevent shear pullout of the threads of the chamber during mechanical tests.

Thread pullout or stripping in threaded connectors is governed by shear stress limits for the materials of the threaded fastener and the nut or section engaged with the fastener. Thus, it is needed only to determine the force required to strip the threads for a given length of thread engagement.[22,23]

The force required to strip the threads is defined as

$$F_{Strip} = USS \times A_S, \tag{5}$$

where *USS* is the ultimate shear strength (typically 0.65 × yield strength) and A_S is the thread shear area for an internal thread. For tests conducted in this system, the maximum load is expected to be about 3.5 kN.

The thread shear area A_S is defined as

$$A_S = \pi n L_E D_{s,\min}\left(\frac{1}{2n} + \tan(30^\circ)(D_{s,\min} - E_{\max})\right), \tag{6}$$

where n is the number of threads per inch, L_E is the length of engagement, $D_{s,\min}$ is the minimum major diameter of the

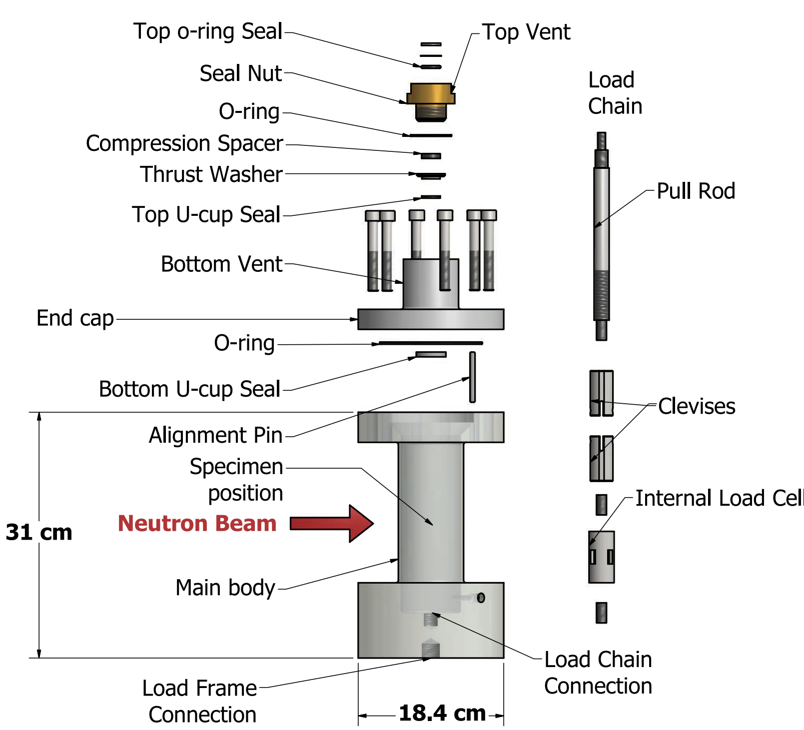

FIG. 1. Schematics of chamber. Fatigue cracks are grown through cyclic actuation of the pull rod. U-cup seals in the chamber end cap prevent leaks as the pull rod slides past the seals.

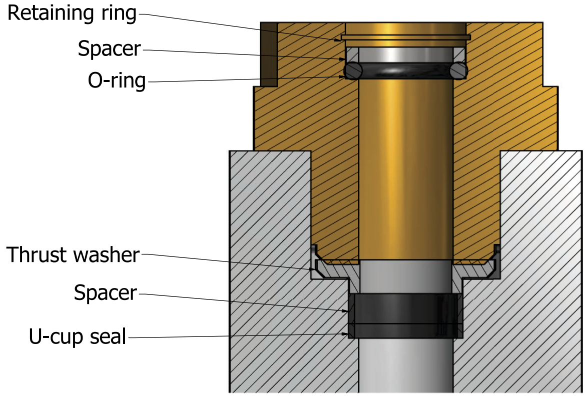

FIG. 2. Schematics of top seal. As the brass seal nut is tightened, the thrust washer and spacer compress the U-cup seal. This causes the U-cup seal to expand around the pull rod, providing a tight seal.

external thread (screw or bolt), and E_{max} is the maximum pitch diameter of the internal thread (nut or flange).

For a length of engagement (load train connecting stud to the chamber) of 1.78 cm (0.7 in.) and a shear strength of 179 kN [=0.65 × 275 MPa (for AA6061-T6)], the force to strip the threads in the chamber is ≈174 kN (39 kip). Similarly for the 1-12 (English units, rather than SI, are used throughout to describe thread sizes) threaded stud that connects the chamber to the load frame, the load necessary to strip the AA6061-T6 threads is 236 kN (53 kip) for an engagement length of 2.29 cm (0.9 in.). These values are greater than the expected nominal operating loads (factors ≈50) and give confidence that under normal operating conditions the threads in the chamber have a sufficient margin of safety, even upon further reduction for other uncertainties in thread specifications, material strength, coefficient of friction, nut dilation, and thread bending.

An aluminum step stud is employed to connect the chamber to the load frame and is designed to strip out at the 3/4-16 threads of the load frame. Similar calculations were used as above, but with the intent to ensure a safe, planned failure mode should take place in the event of an over stroke of the pull rod. It is desirable for the connecting stud threads to fail at the load frame connection, rather than the chamber body, the threads in the chamber, or the threads in the load frame. The thread failure in this instance occurs in the aluminum stud at about 1/4 the load capacity of the load frame threads (which are steel) for a given engagement length. It should be noted here that a minimum stud engagement length of 19 mm (0.75 in.) should be used to establish good alignment for the chamber and load train.

C. Chamber description

Figure 1 shows an exploded view of the schematic of the chamber. The chamber consists of three main sections: the main body, the end cap, and the top seal nut. The main body and end cap sections are made of AA6061-T6, whereas the top seal nut is made of brass. The main body is manufactured as a monolithic chamber from a single rod to provide linear and concentric alignment of the load train, which, in turn, limits minimum wall thickness in the center test section because of manufacturing limitations.

The base of the main body has a threaded hole to allow for mounting to the base of a load frame. A 1/2 in. NPT (National Pipe Thread) port on the side acts as the gas inlet. The reduced section is 17.8 cm tall to allow for sufficient room for equipment at the beamline. The wall thickness was chosen to be 3.175 mm to comply with the minimum wall thickness for the required pressure, as well as the maximum wall thickness to allow neutron transmission. Inside the chamber at the base is a 1/2-20 thread for mounting the load train (Fig. 1, right). Above the reduced test section of the main body, the inside chamber diameter tapers to allow sufficient room for electrical wires associated with gauges for the FCGR measurement. An O-ring seals the connection between the main body and the end cap.

The end cap is attached to the main body with 6 bolts. The base of the end cap has a port with an electrical connector, sealed by two O-rings. The center section of the end cap has two U-cup seals, one at the bottom, which is secured by a brass plate, and one in the narrow section of the end cap, which is secured by the brass seal nut. Between the two seals, a vent resides to release the buildup of gas between the seals as the pull rod is actuated. The top U-cup seal is compressed by a thrust washer. The amount of compression on the thrust washer is controlled by turning the top seal nut.

Figure 2 shows the schematic of the top seal. The top seal nut has an O-ring between its base and the end cap, as well as an O-ring at the interior, where the pull rod sits. Although the inner O-ring does provide a seal, its primary purpose is to maintain proper alignment of the pull rod.

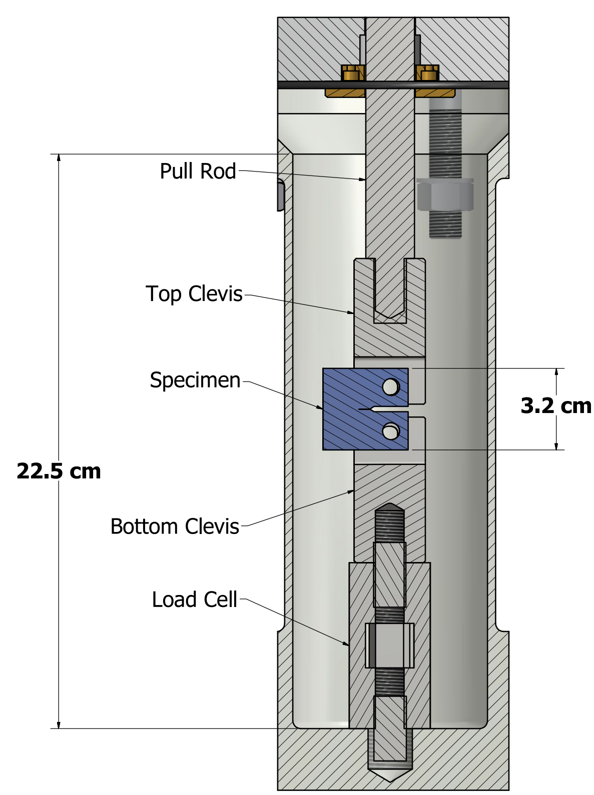

FIG. 3. Load train as it sits within the chamber. The internal load cell provides a measurement of the force on the specimen, once transmitted past the chamber seals. The two clevises are fixed to the specimen, and the cyclic load on the specimen is provided through actuation by the pull rod on the top clevis.

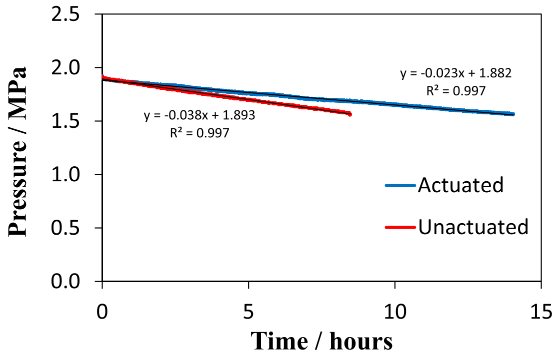

FIG. 4. Chamber pressure as a function of time for both the actuated and unactuated cases.

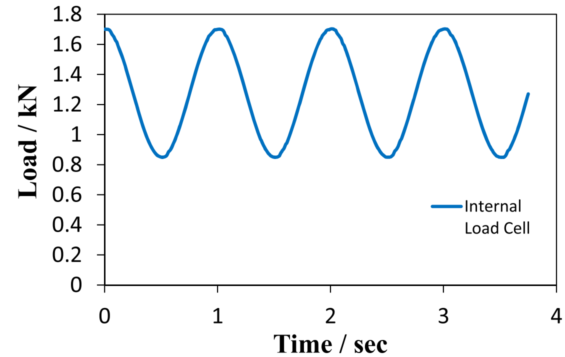

FIG. 5. Load waveform, as measured by the force probe internal to the hydrogen chamber. A clean sinusoidal waveform is achievable even with adequate sealing.

Figure 3 shows the load train as it sits in the chamber. The load train consists of (from the bottom) a load cell, a bottom clevis, the specimen, a top clevis, and a pull rod. The load cell is mounted to the main body, and the bottom clevis is mounted to the load cell, by threaded studs. The pull rod is threaded on the bottom and top to allow for the placement of stop nuts to prevent the pull rod from being pulled out or pushed in past its sealing surface. The pull rod surface is polished to provide adequate sealing.

III. TESTING

A. Leak testing

Leak testing of the chamber was performed at the Hydrogen Facility at NIST, Boulder.[14] The chamber was first pressurized with He to 3.45 MPa. Measurements of the chamber wall outer diameter before and after pressurization indicated negligible expansion of the chamber walls. The chamber was then mounted to the load frame and pressurized with He to 1.9 MPa. The pressure was monitored over the course of 8 h. The pull rod was then actuated for 15 h while the pressure was monitored. Figure 4 shows the pressure as a function of time for both the actuated and unactuated cases. The leak rate during actuation was approximately 0.023 MPa/h. Without actuation of the pull rod, the leak rate was approximately 0.038 MPa/h. Note that the leak rate during actuation is less than the leak rate while the chamber is unactuated. This behavior is consistent with that of the chambers at the NIST Hydrogen Facility and is from the pull rod itself compressing the U-cup seal during actuation.

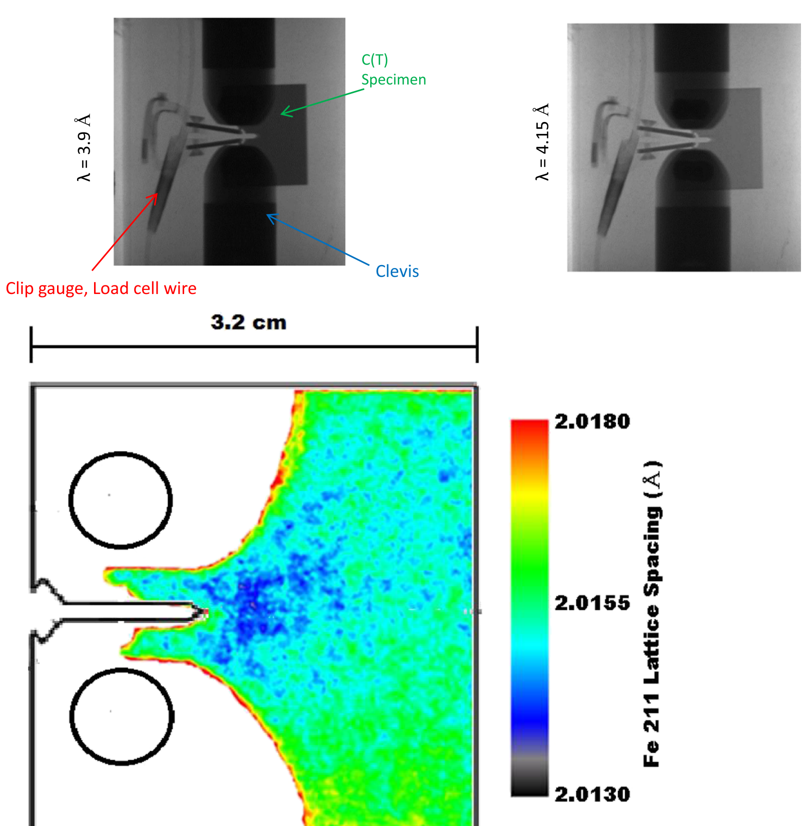

FIG. 6. Neutron radiographs of a fatigue measurement at $\lambda = 3.9$ Å (top) and $\lambda = 4.15$ Å (middle). The transmission as a function of wavelength allowed for the determination of through-thickness lattice spacing through the Bragg edge method (bottom).

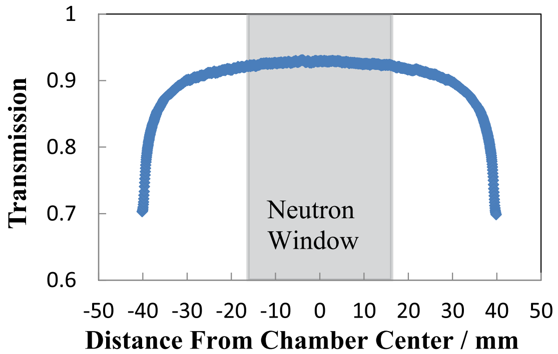

FIG. 7. Transmission of 4 Å neutrons through the chamber as a function of horizontal distance from the center of the chamber. The dips in transmission at ±40 mm are extra attenuation as the beam traverses the edges of the chamber.

B. Mechanical actuation

During actuation, it is crucial that the seals do not impart an excessive friction force on the pull rod, such that a clean cyclic load waveform cannot be achieved. Figure 5 shows the load waveform over a few cycles during the pressure test, as measured by a load cell internal to the chamber. Clearly, the friction due to the seals is not sufficient to prevent the clean sinusoidal waveform required for the FCGR measurements.

C. Neutron imaging

We performed transmission Bragg edge imaging[24] measurements of the strain field near a fatigue crack tip grown in hydrogen. Transmission Bragg edge imaging utilizes Braggs law,

$$\lambda = 2d_{hkl}\sin\theta, \tag{7}$$

where λ is the neutron wavelength, θ is the scattering angle, and d_{hkl} is the lattice spacing corresponding to a specific reflection from the hkl lattice plane. For neutron wavelengths $\lambda > 2d_{hkl}$, Braggs law is not satisfied for any scattering angle θ, and the transmission of neutrons sharply increases as the wavelength is increased above $2d_{hkl}$, the so-called Bragg edge. By measuring the intensity of neutrons incident on a 2D pixelated detector as a function of wavelength, we obtained the distribution of lattice spacings near the crack tip. Figure 6 shows two neutron radiographs measured using incident wavelength below the Bragg edge (Fig. 6, top left) and above the Bragg edge (Fig. 6, top right). For each pixel on the 2D detector, the neutron transmission as a function of wavelength was fit to a function providing an accurate spatial mapping of the lattice spacing (Fig. 6, bottom). The uncertainty in the lattice spacing measurement is estimated to be approximately 10^{-4} Å.

The transmission of a 4 Å neutron beam through the chamber is shown in Fig. 7. At the center of the chamber, the neutron transmission is ≈93%. The transmission of neutrons is within 1% of this maximum value for approximately 16 mm on either side of the chamber center, for a total window size of 32 mm on either side. The drops in transmission at the edges are due to the increased amount of aluminum between the neutron source and the detector at the edges due to the curvature of the chamber.

These measurements demonstrate the feasibility of neutron scattering measurements performed during fatigue cycling using the pressure chamber. We also intend to perform further measurements using synchrotron radiation using the chamber described here. Synchrotron x-ray diffraction from steels tested in air and in H_2 allows for the direct, high-resolution (20 μm) measurements of strain fields, dislocation-density fields, and material phases.[25]

[1] A. J. Slifka, E. S. Drexler, N. E. Nanninga, Y. S. Levy, J. D. McColskey, R. L. Amaro, and A. E. Stevenson, Corros. Sci. **78**, 313 (2014).
[2] N. Nanninga, Y. Levy, E. Drexler, R. Condon, A. Stevenson, and A. Slifka, Corros. Sci. **59**, 1 (2012).
[3] N. Nanninga, A. Slifka, Y. Levy, and C. White, J. Res. Natl. Inst. Stand. Technol. **115**, 437 (2010).
[4] A. Hiriadka *et al.*, "Hydrogen embrittlement of pipeline steels," Ph.D. thesis, Indian Institute of Technology, Bombay, India, 2015.
[5] J. Capelle, J. Gilgert, I. Dmytrakh, and G. Pluvinage, Int. J. Hydrogen Energy **33**, 7630 (2008).
[6] P. P. Darcis, J. McColskey, A. Lasseigne, and T. Siewert, in *Effects of Hydrogen on Materials: Proceedings of the 2008 International Hydrogen Conference, 7-10 September 2008, Jackson Lake Lodge, Grand Teton National Park, Wyoming, USA* (ASTM International, 2009), p. 381.
[7] A. Griesche, E. Dabah, T. Kannengiesser, N. Kardjilov, A. Hilger, and I. Manke, Acta Mater. **78**, 14 (2014).
[8] J. Rowe, K. Sköld, H. Flotow, and J. Rush, J. Phys. Chem. Solids **32**, 41 (1971).
[9] S. Danilkin, H. Fuess, T. Wieder, and A. Hoser, J. Mater. Sci. **36**, 811 (2001).
[10] R. L. Amaro, N. Rustagi, K. O. Findley, E. S. Drexler, and A. J. Slifka, Int. J. Fatigue **59**, 262 (2014).
[11] ASTM Standard , "Standard test method for measurement of fatigue crack growth rates," Technical Report E647-15e1 (ASTM International, West Conshohocken, PA, 2015).
[12] See https://www.ncnr.nist.gov/instruments/bt8/ for "BT8 Residual Stress Diffractometer."
[13] K. An, H. Skorpenske, A. Stoica, D. Ma, X. Wang, and E. Cakmak, Metall. Mater. Trans. A **42**, 95 (2011).
[14] A. Slifka, E. Drexler, R. Amaro, D. Lauria, J. Fekete, and K. Eason, "Materials testing in hydrogen gas at NIST, Boulder," http://www.sandia.gov/matlsTechRef/advmat_presentations/Slifka2_NIST.pdf, 2013, accessed: 10-09-2015.
[15] S. Lovesey and R. Scherm, *Condensed Matter Research Using Neutrons* (Springer, 1984).
[16] See https://www.ncnr.nist.gov/resources/n-lengths/ for "Neutron Scattering Lengths and Cross Sections."
[17] X. Tan, P. Conway, and F. Sarvar, J. Mater. Process. Technol. **168**, 152 (2005).
[18] C. L. Yaws and W. Braker, *Matheson Gas Data Book* (McGraw Hill Professional, 2001).
[19] M. Sadd, *Elasticity: Theory, Applications, and Numerics* (Academic Press, 2014).
[20] C. Chantler, J. Phys. Chem. Ref. Data **29**, 597 (2000).
[21] V. Sears, Neutron News **3**, 26 (1992).
[22] J. Bickford, *Handbook of Bolts and Bolted Joints* (CRC Press, 1998), pp. 135–138.
[23] E. Oberg, F. Jones, H. Horton, H. Ryffel, and J. Geronimo, *Machinery's Handbook* (Industrial Press, New York, 2004), Vol. 200, pp. 1510–1511.
[24] J. Santisteban, L. Edwards, M. Fitzpatrick, A. Steuwer, P. Withers, M. Daymond, M. Johnson, N. Rhodes, and E. Schooneveld, Nucl. Instrum. Methods Phys. Res., Sect. A **481**, 765 (2002).
[25] P. Withers and P. Webster, Strain **37**, 19 (2001).